Ferroelectricity in Strain-Free SrTiO₃ Thin Films

H. W. Jang,[1] A. Kumar,[2] S. Denev,[2] M. D. Biegalski,[3] P. Maksymovych,[3] C. W. Bark,[1] C. T. Nelson,[4] C. M. Folkman,[1]
S. H. Baek,[1] N. Balke,[3] C. M. Brooks,[2,5] D. A. Tenne,[6] D. G. Schlom,[5] L. Q. Chen,[2] X. Q. Pan,[4] S. V. Kalinin,[3]
V. Gopalan,[2] and C. B. Eom[1,*]

[1]*Department of Materials Science and Engineering, University of Wisconsin, Madison, Wisconsin 53706, USA*
[2]*Department of Materials Science and Engineering, Pennsylvania State University, Pennsylvania 16802, USA*
[3]*Center for Nanophase Materials Sciences, Oak Ridge National Laboratory, Oak Ridge, Tennessee 37831, USA*
[4]*Department of Materials Science and Engineering, University of Michigan, Ann Arbor, Michigan 48109, USA*
[5]*Department of Materials Science and Engineering, Cornell University, Ithaca, New York 14853, USA*
[6]*Department of Physics, Boise State University, Boise, Idaho 83725-1570, USA*
(Received 24 November 2009; published 13 May 2010)

Biaxial strain is known to induce ferroelectricity in thin films of nominally nonferroelectric materials such as SrTiO₃. By a direct comparison of the strained and strain-free SrTiO₃ films using dielectric, ferroelectric, Raman, nonlinear optical and nanoscale piezoelectric property measurements, we conclude that all SrTiO₃ films and bulk crystals are relaxor ferroelectrics, and the role of strain is to stabilize longer-range correlation of preexisting nanopolar regions, likely originating from minute amounts of unintentional Sr deficiency in nominally stoichiometric samples. These findings highlight the sensitive role of stoichiometry when exploring strain and epitaxy-induced electronic phenomena in oxide films, hetero-structures, and interfaces.

Pure SrTiO₃ (STO) is a quantum paraelectric material where quantum fluctuations of atomic positions suppress a ferroelectric transition, leading to a so-called incipient ferroelectric [1–4]. Surface ferroelectricity in a few mono-layers of SrTiO₃ has been predicted and observed [5–7]. Bulk piezoelectricity and ferroelectricity in the volume of SrTiO₃ can be induced by Ca doping [8], electric field [3,9], mechanical stress [10], and ^{18}O substitution [11] in the low-temperature regime. It has been demonstrated that tensile-strained commensurate epitaxial STO films can be ferroelectric at room temperature [12,13]. However, a recent study shows that strained STO films on DyScO₃ are relaxor ferroelectric, likely due to Sc doping [14]. Furthermore, STO films grown on (001) STO substrates under low oxygen pressures have been observed to be ferroelectric at room temperature owing to the unusual tetragonality and increased unit cell volume [15]. Therefore, the precise nature of strain-induced ferroelectricity in STO films is still unclear, with variously cited roles of strain, doping, abnormal cell volumes in a range of films deposited on different substrates and under different conditions.

In this Letter, we shed light on the nature of strain-induced ferroelectricity in well-controlled, normal unit cell volume, STO single crystal films. A direct comparison between 1.18% compressively strained and strain-free STO epitaxial thin films has been performed through temperature-dependent capacitance, ferroelectric polariza-tion, optical Raman and second harmonic generation, and piezoresponse force microscopy (PFM) measurements. We conclude that strained and strain-free films, as well as single crystals of STO are relaxor ferroelectrics to varying degrees.

(001) STO films were grown on (110) NdGaO₃ (NGO) and (001) STO substrates using pulsed-laser deposition (PLD) with *in situ* reflection high-energy electron diffrac-tion. The pseudocubic in-plane lattice parameters of the NGO substrate are 3.863 ± 0.0015 Å and 3.854 ± 0.0015 Å. This corresponds to an average biaxial compres-sive strain of ~1.18% in a fully commensurate STO film on the substrate. We used lattice-matched $Sr_{0.2}Ca_{0.8}RuO_3$ (SCRO) bottom and top electrodes on NGO [16]. On SCRO/NGO substrates, 60 nm thick strained STO films were grown, which were thick enough for electrical mea-surements. The full width at half maximum (FWHM) of the strained STO films is as small as $0.003 \pm 0.0005°$, which is much narrower than that of the bulk STO single crystal. For strain-free STO films on STO with a 50 nm thick SrRuO₃ (SRO) bottom electrode, the volume of the films is measured to be same as that of the substrate, which provides evidence that the PLD-grown STO films are free from excessive point defects as is likely the case in the previous report [15]. The surface of films was atomically smooth with single unit cell height steps measured by atomic force microscopy (AFM).

Temperature-dependent capacitance data of the strain-free STO film in Fig. 1(a) are well fit by the Curie-Weiss law, $\varepsilon(T) \propto (T - T_C)^{-1}$, where ε is the dielectric constant, consistent with bulk single crystals. The 60 nm thick strained film on NGO exhibits maximum capacitances at 120–140 K, well within the theoretically predicted tem-perature range of 80–230 K [12]. The temperature T_m of the ε maximum is shifted to higher values at higher frequencies. This strong dielectric dispersion is evi-dence leading to a Vogel-Fulcher behavior described by

$f = f_0 \exp[-E_a/k_B(T_m - T_f)]$ where f_0 is the attempt frequency, E_a the activation energy, k_B the Boltzmann constant, and T_f the static freezing temperature. $T_m(f)$ of the strained STO is well fit with $T_f = 85$ K, $E_a = 0.081$ eV, and $f_0 = 4.0 \times 10^{12}$ Hz. The E_a and f_0 are reasonable values for typical relaxor behavior [17].

The temperature-dependent polarization of both the strained and strain-free STO films is plotted in Fig. 1(b). Negligible remanent polarization (P_r) is detected in the strain-free film, whereas the strained film displays a ferro-electric polarization-electric field hysteresis loop with the P_r of ~ 9.5 μC/cm^2 at 7 K. The gradual decease of P_r below T_m is different from normal ferroelectrics including

BiFeO$_3$ (BFO) which shows an abrupt drop in polarization at the ferroelectric transition [18]. Temperature-dependent optical second harmonic generation (SHG) measurements as shown in Fig. 1(c). For the strained film, no SHG was observed from the NGO substrate or the SCRO bottom electrode. The SHG signal was thus attributed only to the STO film. Compared with a STO single crystal, the strained STO film shows stronger SHG signal at room temperature and a strong temperature dependence. Similar to P_r, the SHG signal decreases gradually with increasing temperature, which is significantly different from normal ferroelectric BaTiO$_3$ [19]. An important thing to note is that finite SHG signal still exists even at room temperature for both the film and bulk single crystal, indicating the presence of nanopolar regions in both [20].

Domain writing or reading or hysteresis loops by PFM are widely used to check whether thin films are ferroelec-tric [21]. Since PFM signal arises from a ~ 100 nm volume under the tip, these measurements on our 50 nm thick films are volume responses. Figure 2(a) shows amplitude-contrast PFM image after applying -12 V to 2.5×2.5 μm^2 area for a strained STO film on NGO at room temperature. The larger piezoresponse signal of the poled region clearly indicates the feasibility of domain writing/reading by PFM even at room temperature well above T_m. For strain-free STO films, there was no signature of poling observed in the slow domain writing and subsequent read-ing process which typically takes 10–30 min each. However, the PFM contrast for the strained STO film gets weaker with time [Fig. 2(a)] and completely disap-peared after 4 h. This suggests that the field-induced long-range correlation between preexisting nanopolar regions thermally decays with time in the strained STO film. Autocorrelation maps of these images were calculated following a procedure outlined earlier [22]. The average autocorrelation function versus distance in Fig. 2(b) shows that the correlation length, ξ, under electric fields can extend up to >1000 nm (similar to the size of the written domain pattern), and it collapses to <100 nm (noise floor) over 4 h after the removal of the field.

Figure 2(c) shows PFM hysteresis loops with short and long pulse-off duration times for strain-free and strained STO films. The strained film shows significantly enhanced ferroelectric hysteresis loops, but even the strain-free film shows ferroelectric hysteresis loops. With longer pulse-off duration, the loops degrade. Thus, a time-dependent decay of the PFM signal, which is proportional to the net polar-ization, is observed in both the PFM domain writing or reading and hysteresis loop measurements. To confirm the decay of the PFM signals, we have measured the PFM signal as a function of time after poling at -25 V for both films, as plotted in Fig. 2(d). The strained film shows a larger signal and a much slower decay, whereas the un-strained STO shows a rapid decay of the PFM signal. The lack of PFM signal from a mica sample, for example,
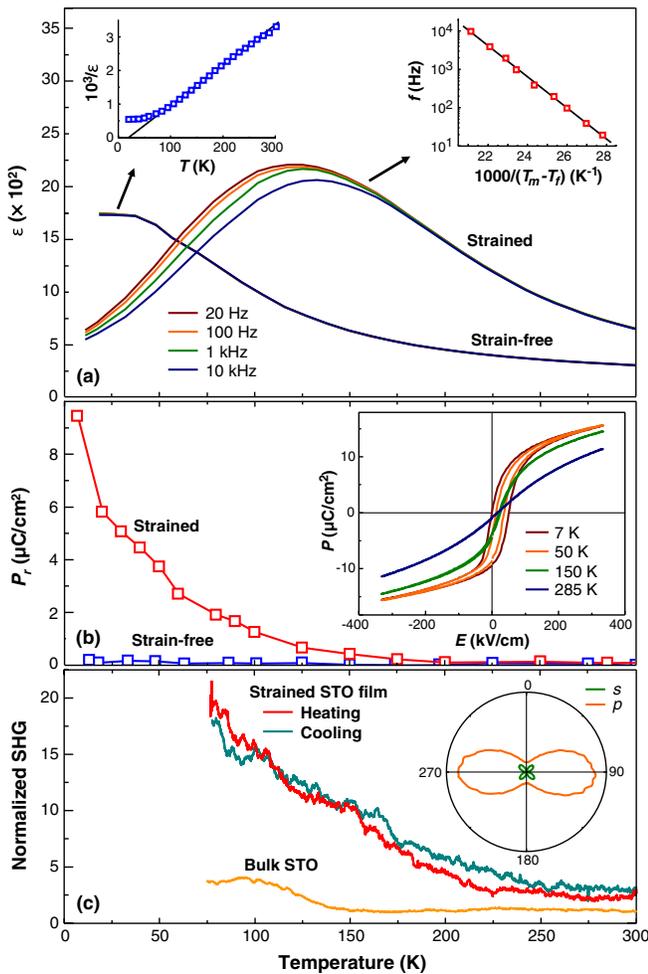

FIG. 1 (color online). (a),(b) Temperature dependence of (a) dielectric constant and (b) remanent polarization for a 60-nm-thick STO film on NGO (strained) and a 100-nm-thick STO film on STO (strain-free). (c) SHG signals for the strained STO film and a STO single crystal. The latter is magnified ~ 12 times for clarity. The SHG vs temperature of a 100 nm STO film on STO is indistinguishable from the SHG of a (100) STO single crystal. Insets: (a) fits to the Curie-Weiss law and the Vogel-Fulcher law, (b) P-E hysteresis loops of the strained film, and (c) SHG polar plots show tetragonal symmetry.
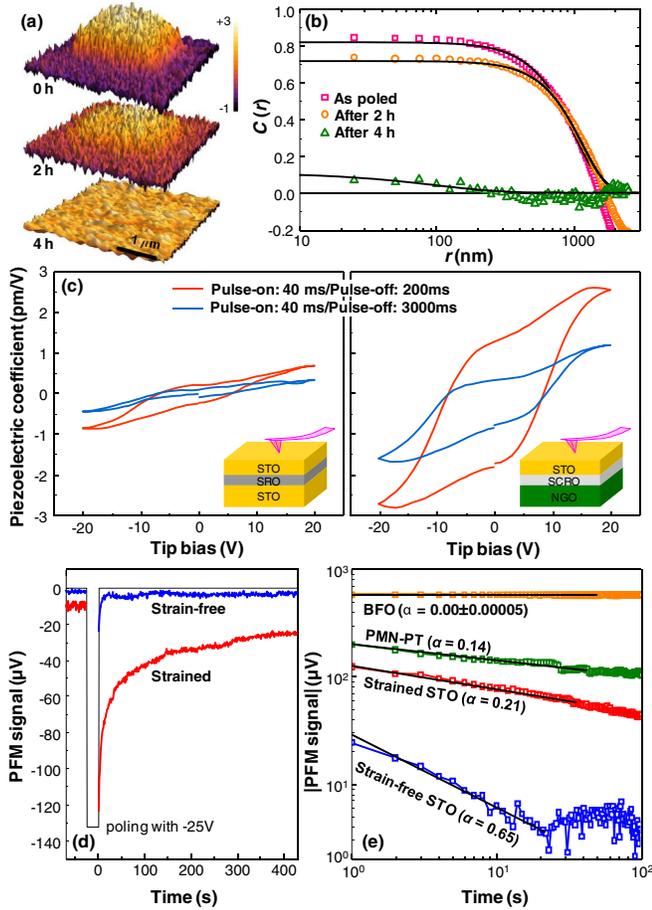
FIG. 2 (color online). (a) Amplitude-contrast PFM images as
poled (0 h), after 2 h, and after 4 h for a 50-nm-thick strained
STO film on NGO. (b) Correlation function, $C(r) = \sum_r I(r + \Delta r)I(r)$, calculated for (a) as a function of distance in the y direction. The solid lines are fits to $C(r) = \sigma^2 \exp(-(r/\xi)^{2h})$,
where (σ, ξ, h) for 0, 2, and 10 h are, respectively, (~ 0.82,
~ 1044, ~ 2.25), (~ 0.71, ~ 1164, ~ 2.37), and (~ 0.11, ~ 100,
~ 0.91). (c) PFM hysteresis loops for 50-nm-thick strain-free and
strained STO films. The loops are measured at room temperature
in air with a 100 nm biased tip by applying voltage pulses of
40 ms for domain reversal, followed by variable pulse-off
periods during which time the PFM signal is measured to avoid
electrostatic contributions. (d) Change of PFM signal before and
after poling with -25 V. (e) PFM signal as a function of time
after poling with -25 V for BFO, PMN-PT, strained, and strain-
free STO films. Solid black lines are fits to the power-law decay.

implies that the behavior is not due to charge injection or
other artifacts from surface interaction.

The gradual decay of the PFM signals has been fit to the
power-law decay equation, $P(t) = P_0 t^{-\alpha}$, where P_0 is the
magnitude of the initial PFM signal and α the decay
exponent. The linear behavior in $\log[P(t)]$ versus $\log[t]$
plots in Fig. 2(e) verifies that the decay of the PFM signals
in both STO films on NGO and STO follow the power-law
behavior at room temperature, meaning that the decay of
the PFM signals is a thermal process. The smaller slope, α,
of the strain-free film corresponds to the higher stability of

the field-induced local ferroelectricity. In contrast, the
normal ferroelectric BFO film on (001) STO (with a T_C
of 830 °C) [23] shows no decay in PFM signal for the
measured time period, while the relaxor
$0.67Pb(Mg_{1/3}Nb_{2/3})O_3 - 0.33PbTiO_3$ (PMN-PT) film on
(001) STO [24] shows decay, and its behavior is analogous
to that of the strained STO film. These results, as well as
the observation of the gradual decay of local contrast (as
opposed to the domain-wall driven contraction), suggest
that the decay of the PFM signal reflects the relaxor nature
of the material. Since the PFM signal is free from polar-
ization relaxation by backswitching due to the depolariza-
tion effect [25,26], the P_0 and α values are intrinsic
properties. Whether the material is a normal ferroelectric
or a relaxor is reflected by the α value.

In order to rule out extrinsic effects of surface electro-
chemistry [27] or charge injection (electret effect) medi-
ated by mobile ions in the ambient atmosphere, we have
carried out control PFM measurements under ultrahigh
vacuum (2×10^{-10} Torr) at 50 K–300 K. The measure-
ments confirm the presence of switchable polarization on
the strained film, and very weak ferroelectric hysteresis on
the strain-free film, in qualitative agreement with the
ambient measurements in Fig. 2. At 50 K, we have been
able to pole both STO films [Figs. 3(a) and 3(b)] and the
polarization domain patterns were stable on at least 30 min
time scale.

Our experimental results strongly indicate that both
strain-free and strained STO films exhibit relaxor behavior
at low temperatures. The origin of the relaxor behavior
should be nanopolar regions as suggested by Fig. 1(c).
Figure 4(a) shows the Raman spectra of five different
material systems based on STO. The key result is the
appearance of first order Raman scattering by polar modes
(TO_2, LO_3, TO_4, and LO_4) in all the film systems. The
$SrTiO_3$ single crystal also shows weak signatures of TO_2
and TO_4 modes, which is consistent with the SHG signal
and indicates weak polar nature. The polar modes are weak
in the nearly stoichiometric MBE film, and are the stron-
gest in the nonstoichiometric $Sr_{0.9}TiO_{3-x}$ film, which has
intentionally introduced Sr deficiency. The 50 nm thick
STO film of this study also exhibit strong polar modes.
Nearly identical behavior is observed in the 1 μm thick
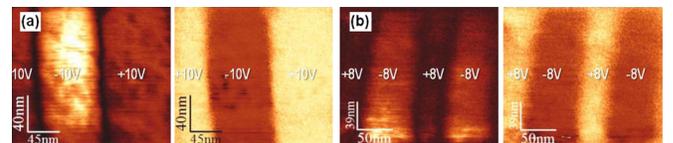film. The temperature evolution of Raman spectra

FIG. 3 (color online). Vacuum PFM images (left:
amplitude contrast, right: phase contrast) of polarization do-
mains recorded at 50 K by scanning the tip biased at
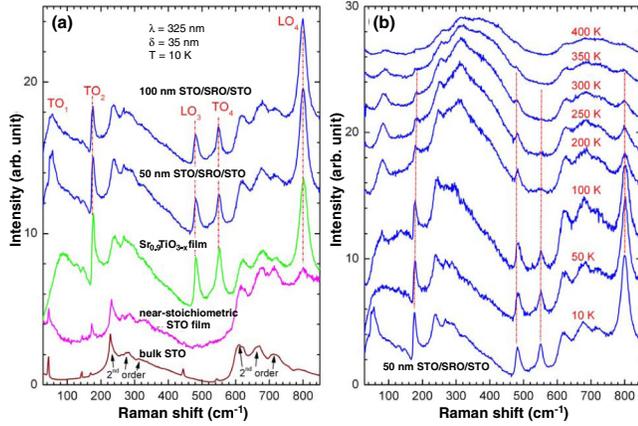± 8–10 V across the surface of the (a) strain free and (b) strained
STO films.

FIG. 4 (color online). (a) Raman spectra of a bulk STO single crystal, a near-stoichiometric STO film grown on STO by molecular-beam epitaxy (MBE), an intentionally Sr-deficient film with composition $Sr_{0.9}TiO_{3-x}$ grown on STO by MBE, and nominally stoichiometric 50 and 1000 nm thick STO films grown on SRO/STO by PLD at 10 K. (b) Temperature-dependent Raman spectra of the 50 nm thick STO/SRO/STO film.

[Fig. 4(b)] clearly indicates that the films remain polar up to $\sim$350 K, which is consistent with the optical and PFM observations. Chemical composition analysis by wavelength dispersive x-ray spectroscopy on the 1 μm thick STO film indicates that the film has a Sr/Ti ratio of $\sim$0.97, which is stoichiometric within experimental error. These findings indicate that the most likely reason for the ferroelectricity is a small amount of Sr deficiency in our nominally stoichiometric STO films. A clear distinction between STO and previously reported relaxor systems by A-site cation doping [28–31] is that STO has only Sr on the A site with minute amounts of unintentional Sr deficiency.

In conclusion, we demonstrate relaxor ferroelectricity in the volume of strain-free STO films consisting of nanopolar regions with short correlation lengths. The role of strain is, in a sense, similar to an electric field, in that both can stabilize long-range correlation between preexisting nanopolar regions. The power-law exponent, α as well as the time dependence of the correlation length, ξ, as measured from the decay of the PFM signal are good measures to evaluate the nature of ferroelectricity in thin films. There is tremendous interest in $SrTiO_3$ today such as for 2D electron gases of $LaAlO_3/SrTiO_3$ [32] and in strain-induced ferroelectricity [33]. This study highlights the importance of relaxor ferroelectricity arising from minute amounts of nonstoichiometry even in nominally stoichiometric STO single crystals and unstrained films. Finally, we propose that strain-induced relaxor ferroelectricity can exist in other ABO_3 incipient ferroelectrics such as $KTaO_3$ and $CaTiO_3$ based on a similar mechanism.

*eom@engr.wisc.edu

[1] K. A. Müller and H. Bukard, Phys. Rev. B **19**, 3593 (1979).
[2] W. Zhong and D. Vanderbilt, Phys. Rev. B **53**, 5047 (1996).
[3] J. H. Barrett, Phys. Rev. **86**, 118 (1952).
[4] J. Hemberger et al., Phys. Rev. B **52**, 13 159 (1995).
[5] N. Bickel, G. Schmidt, K. Heinz, and K. Muller, Phys. Rev. Lett. **62**, 2009 (1989).
[6] V. Ravikumar, D. Wolf, and V. P. Dravid, Phys. Rev. Lett. **74**, 960 (1995).
[7] R. Herger et al., Phys. Rev. Lett. **98**, 076102 (2007).
[8] T. Mitsui and W. B. Westphal, Phys. Rev. **124**, 1354 (1961).
[9] P. A. Fleury and J. M. Worlock, Phys. Rev. **174**, 613 (1968).
[10] W. J. Burke and R. J. Pressley, Solid State Commun. **9**, 191 (1971).
[11] M. Itoh et al., Phys. Rev. Lett. **82**, 3540 (1999).
[12] J. H. Haeni et al., Nature (London) **430**, 758 (2004).
[13] M. P. Warusawithana et al., Science **324**, 367 (2009).
[14] M. D. Biegalski et al., Appl. Phys. Lett. **88**, 192907 (2006).
[15] Y. S. Kim et al., Appl. Phys. Lett. **91**, 042908 (2007).
[16] C. B. Eom et al., Science **258**, 1766 (1992); D. L. Proffit et al., Appl. Phys. Lett. **93**, 111912 (2008).
[17] D. Viehland et al., J. Appl. Phys. **68**, 2916 (1990).
[18] S. M. Selbach et al., Adv. Mater. **20**, 3692 (2008).
[19] K. J. Choi et al., Science **306**, 1005 (2004).
[20] A. Vasudevarao et al., Phys. Rev. Lett. **97**, 257602 (2006); S. Denev et al., Phys. Rev. Lett. **100**, 257601 (2008).
[21] A. Gruverman, O. Auciello, and H. Tokumoto, Annu. Rev. Mater. Sci. **28**, 101 (1998).
[22] V. V. Shvartsman and A. L. Kholkin, J. Appl. Phys. **101**, 064108 (2007).
[23] H. W. Jang et al., Phys. Rev. Lett. **101**, 107602 (2008).
[24] S. D. Bu et al., Appl. Phys. Lett. **79**, 3482 (2001).
[25] D. J. Kim et al., Phys. Rev. Lett. **95**, 237602 (2005).
[26] D. D. Fong et al., Phys. Rev. Lett. **96**, 127601 (2006).
[27] S. V. Kalinin, A. Rar, and S. Jesse, IEEE Trans. Ultrason. Ferroelectr. Freq. Control **53**, 2226 (2006).
[28] A. K. Tagantsev et al., Phys. Rev. B **65**, 012104 (2001).
[29] M. Tyunina et al., Phys. Rev. B **74**, 104112 (2006).
[30] M. Tyunina et al., J. Appl. Phys. **101**, 084119 (2007).
[31] S. Glinšek et al., Appl. Phys. Lett. **94**, 172905 (2009).
[32] A. Ohtomo and H. Y. Hwang, Nature (London) **427**, 423 (2004).
[33] J. H. Haeni et al., Nature (London) **430**, 758 (2004).